Chirp Signal Denoising Based on Convolution Neural Network

Ben Guangli (g2009051126@163.com)
Changchun Institute of Optics Fine Mechanics and Physics Chinese Academy of Sciences
https://orcid.org/0000-0002-9418-0641

Xifeng Zheng
Changchun Institute of Optics Fine Mechanics and Physics Chinese Academy of Sciences

Yongcheng Wang
Changchun Institute of Optics Fine Mechanics and Physics Chinese Academy of Sciences

Xin Zhang
Changchun Institute of Optics Fine Mechanics and Physics Chinese Academy of Sciences

Ning Zhang
Changchun Institute of Optics Fine Mechanics and Physics Chinese Academy of Sciences

Research

Keywords: Chirp signal, Deep leaning Denoising, Chirp parameter estimation

Posted Date: May 13th, 2020

DOI: https://doi.org/10.21203/rs.3.rs-27563/v1

Chirp Signal Denoising Based on Convolution Neural Network

Guangli Ben*, Xifeng Zheng, Yongcheng Wang, Xin Zhang, Ning Zhang

Changchun Institute of Optics, Fine Mechanics and Physics, Chinese Academy of Science
Changchun 130033, China

Abstract

Many classical chirp signal processing algorithm may experience distinct performance decrease in noise circumstance. To address the problem, this paper proposes a deep learning based approach to filter noises in time domain. The proposed denoising convolutional neural network (DCNN) is trained to recover the original clean chirps from observation signals with noises. Following denosing, we employ two parameter estimation algorithm to DCNN output. Simulation result show that the proposed DCNN method improves the signal noise ratio (SNR) and parameter estimation accuracy to a great extent compared to the signals without denoising. And DCNN have a strong adaptability of low SNR input scenarios that never trained.

Keywords: Chirp signal, Deep leaning Denoising**,** Chirp parameter estimation

1 Introduction

Chirp signals have a broad range of applications, such as in radar, sonar, communication and medical imaging [1]. Chirp usage and estimation of their parameters is a significant part in the digital signal processing area [2]. At present, directly use the time–frequency based methods have been practiced to be effective for detecting and estimating chirp signals. But whose accuracy is closely related to the SNR level and most of them cannot reconstruct the clean signals in time domain. This paper is focus on filtering noises by DCNN at low SNR scenarios in time domain and evaluating the filter performance by comparing the parameter estimation accuracy and SNR improvement.

Data driven for filtering noise and estimating parameter methods have been of significant interest in recent years. Yuan Jiang proposed a deep learning denoising based approach for line spectral estimation [3], by using convolutional neural network (CNN) to filter noises of sinusoidal signals in time domain and offers a substantial improvement in line spectral estimation, but which training data and validation data are under SNR =15, 20, 25, 30, 35, 40dB, the bandwidth of test signals are narrowed, and do not discuss the extend adaptability of CNN. Besides denoising in time domain, Se Rim Park proposed a method to remove noise from speech signals for enhancing the quality and intelligibility of speech in time-frequency domain [4], the training date and validation data are the magnitude spectra of the noisy and clean audio signals respectively, the network's output is the magnitude spectrum of the denoised signal, and then converted back to the time domain using the output magnitude spectrum and the phase of the noisy signal. Xiaolong Chen applies CNN for replacing the Fourier transform and Fractional Fourier transform (FrFT), uses it for single frequency signal and LFM signal detection and estimation [5], it have proved that the CNN based method can achieve good recognition performance at SNR above -2dB, and above -10dB combined with the wavelet denoising method. CNN also plays an active role in the field of signal detection and classification. Huyong Jin proposed a CNN based framework to perform preamble detection for underwater acoustic communications application [6], which can learns features from the time-frequency spectrum, and can gives an efficient solution for preamble detection under complicated underwater acoustic communications. For signal classification, Johan Brynolfsson uses Wigner-Ville distribution instead of the spectrogram as basic input into CNN to Classify One-Dimensional Non-Stationary Signals and has achieved good performance [7].

Following with above ideas, this paper proposes a deep learning denoising based method for improving chirp signal's SNR and parameter estimation accuracy in low SNR environments. The proposed method consists of a DCNN, which is trained to perform filtering noises in time domain, and a parameter estimation process applied on the denoised signal to evaluate DCNN performance. Moreover the potential adaptability of DCNN in low SNR environments is

also discussed.

Assum a chirp signal $x_i(t)$ with Additive Gaussian noise $n(t)$ is modeled as:

$$y_i(t) = x_i(t) + n(t) \quad (1)$$

Where $x_i(t) = \sin(2\pi f_0 t + \pi k t^2)$, f_0 denotes the initial frequency, k denotes the chirp rate, the prior knowledge of their value are unknown. We employ DCNN to extract denoised signals $\hat{y}$ from observation $y_i(t)$, and then evaluate DCNN performance by calculating the SNR and parameters of $\hat{y}$.

This paper is organized as follows. Section 2 introduces the DCNN structure with associated inner layer details. And briefly provides reviews on Radon-Wigner Ville transform (RW) and FrFt method used for parameter estimation. In Section 3, simulation results are given to show the advantages of the DCNN. Finally, conclusions drawn in Section 4

2 Method

2.1 DCNN Construction

The proposed DCNN has a layer structure as described in Fig.1, totally consists of 34 layers. Input layer receives the observation Y^0, and $Y^0 = \{y_1(t), y_2(t), \ldots y_M(t)\}$, M is mini-batch size, $y_i(t)$ is the observation noised chirp signal with N points, and reshaped into a N×1×1 tensor.

Layer1 to Layer30 have a Conv+BN+Tanh structure. Each Conv layer consists of K convolutional kernels and K=64, 32, or 8, the kernel size is 8x1. Conv layer applies sliding convolutional filters to the input Y^{i-1} by moving the kernels along Y^{i-1}, and compute the product of input Y^{i-1} and weights W^i, then adding bias term B^i. Convolution output G^i can be expressed as:

$$G^i = Y^{i-1} * W^i + B^i \quad (2)$$

Where i denote the layer number, W^i and B^i are learnable parameters, Y^{i-1} is output of Layeri-1. The dimension of G^i is Nx1xK, as the convolution is operated with same padding.

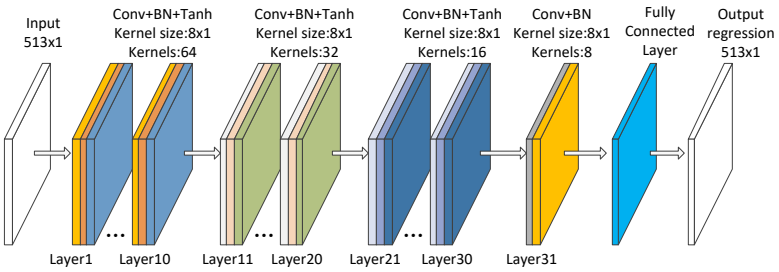

Fig.1. Structure of DCNN

BN layer normalize its input G^i in order to speed up training and reduce the sensitivity to DCNN [8]. BN first calculating the mean μ and variance δ^2 across a mini-batch over each input G^i. Then, the normalized activations can be described as:

$$\hat{G}^i = \frac{G^i - \mu}{\sqrt{\delta^2 + \varepsilon}} \quad (3)$$

Hyper parameter ε is set to 0.00001, to improve numerical stability when mini-batch variance is too small. Then BN shift and scale the activations as:

$$Z^i = \lambda \hat{G}^i + \beta \quad (4)$$

where λ is scale factor, β is offset, they are learnable parameters.

After BN normalization, we use a nonlinear activation function hyperbolic tangent (tanh) to increase nonlinear properties of DCNN, and then Layeri output Y^i can be expressed as:

$$Y^i = \tanh(Z^i) = \frac{e^{z^i} - e^{-z^i}}{e^{z^i} + e^{-z^i}} \quad (5)$$

Because the additive white Gaussian noise (WGN) is randomly distributed along the clean signal, each observation Y^0 with the same SNR may have different value at same point. In order to train DCNN to effectively remove noises from observation Y^0, we need a large amount of training signals with approximate SNR. The initial frequency f_0 and chirp rates k of the training signals are generated at an interval of 1 over a range, which covers the signals of interest. Here assume the prior knowledge of their range is available. Each SNR we added to clean signal is not strictly match to a fixed value, which is approximately at an interval of 1 over a range. We randomly generate a number of training signals with the same parameter around an approximate SNR. The validation data are clean signals with

the same parameter as training data. We shuffle the training data before each training epoch, and validation data before each network validation.

In our proposed scheme, DCNN is trained to remove noises from training data set and output the denoised signal $\hat{Y}$, The optimization goal of training is to minimize the half-mean-squared-error loss between $\hat{Y}$ and the clean labels X. The loss function is given by:

$$\text{loss} = \frac{1}{2}\sum_{i=1}^{M}(\hat{Y}^i - X^i)^2 \quad (6)$$

where M is the number of output responses. During training process, we use mini-batch gradient descent with Adam optimization algorithm [9] to evaluate the gradient of the loss function and update DCNN weights. In our test, we use Matlab Deep Learning Toolbox to train DCNN.

2.2 Parameter Estimation Algorithm Employed

After denoising, the initial frequency f_0 and chirp rate k of observation Y are estimated by denosied output $\hat{Y}$. Many parameter estimation method are available, such as the method based on maximum likelihood principle [10],[11],[12], based on using the gradient of the short-time Fourier transform complex phase [13], based on Fractional Order Cross Spectrum [14] and so on. For our problem, we choose RW [15],[16] and FrFT [17],[18] methods to estimate chirp parameters.

For a chirp signal y with duration T, the Wigner Ville distribution (WVD) is:

$$WVD(t,f) = \int_{-T/2}^{T/2} y(t+\tau/2)y^*(t-\tau/2)\,e^{-j2\pi f\tau}d\tau \quad (7)$$

The $WVD(t,f)$ shape of chirp signal in time-frequency plan is like a linear dorsal fin as shown in Fig.6.

In order to estimate parameters, we do a Radon transform for $WVD(t,f)$ (RW), as shown in Fig.2, the linear integral is along the line PQ at different radius ρ and angle θ, witch can be described in the following formula:

$$\text{RW}(\rho,\theta) = \int WVD(u\cos\theta - v\sin\theta, u\sin\theta + v\cos\theta)dv \quad (8)$$

Radon transform converts time-frequency plan to u-v plan. In u-v plan we extract linear component by searching the maximal amplitude of RW(ρ, θ) at rotation angle θ' and integral radius ρ', which correspond to the linear time-frequency distribution of y. Then we can get the estimation result as follows:

$$\{\rho', \theta'\} = \arg\max_{\rho,\theta}\{RW(\rho,\theta)\} \quad (9)$$

$$\hat{k} = -\cot\theta' \quad (10)$$

$$\hat{f}_0 = \rho'/\sin\theta' \quad (11)$$

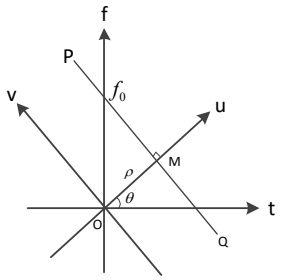

Fig.2. The diagram of Radon transform

The inverse FrFT of a finite signal y(t) is defined as follows:

$$\text{y(t)} = \int_{-\infty}^{+\infty} Y_p(u)K_{-p}(t,u)dt \quad (12)$$

Where $\text{Y}_\text{p}(\text{u})$ is the FrFT of y(t), p is FrFT order, $\text{K}_\text{p}(\text{t},\text{u})$ is FrFT kernel function and it is defined as:

$\text{K}_\text{p}(\text{t},\text{u}) =$

$$\begin{cases} \sqrt{\dfrac{1-j\cot\alpha}{2\pi}}\exp\left[j\left(\dfrac{u^2+t^2}{2}\cot\alpha - ut\csc\alpha\right)\right] & \alpha \neq n\pi \\ \delta(t-u) & \alpha = 2n\pi \\ \delta(t+u) & \alpha = (2n+1)\pi \end{cases} \quad (13)$$

Where α is FrFT rotation angle, and $\alpha = \text{p}\pi/2$.

The above formula explains that y(t) is a summation based on inverse kernel space $\text{K}_{-\text{p}}(\text{t},\text{u})$, the coefficients are $\text{Y}_\text{p}(\text{u})$. And $\text{K}_{-\text{p}}(\text{t},\text{u})$ can be represented as a set of orthogonal chirps in u domain. So the FrFT of a chirp signal at an appropriate order will be represented as a pulse. And Gauss noises do not have this feature. In other words, FrFT have a good property of energy aggregation for chirp signal at corresponding order p. So, by searching the maximal amplitude of FrFT at u_0 and α_0, we can calculate chirp parameter as follows:

$$\{u_0, \alpha_0\} = \arg\max_{u,\alpha}\{abs(Y_p(u))\} \quad (14)$$

$$\hat{f}_0 = u_0\csc\alpha_0 \quad (15)$$

$$\hat{k} = -\cot\alpha_0 \quad (16)$$

3 Simulation Results and Discussion

In our simulation, chirp signal sample frequency is 256Hz, duration is 2 seconds. The range of initial frequency f_0 is from 15Hz to 20Hz at an interval of 1Hz, and the range

of chirp rate is from 5Hz/s to 10Hz/s at an interval of 1Hz/s. There are 5 SNR levels generated by matlab awgn function with signal power in measured mode, the range of SNR is about from -13dB to -9dB at an interval of 1dB. At each SNR we randomly generate 800 training signals and 150 validation signals. The training data set size is 144000 signals. Validation data set size is 27000 signals.

We use mini-batch gradient descent method to update DCNN parameters, and each mini-batch size is 128. Maximum number of epochs is 8, so there are 8 full passes of the training algorithm over entire training set, and before each training epoch we shuffle the training data. Validation frequency is set to 562 iterations, so each epoch we validate two times, and before each validation we shuffle the validation data too. The initial learning rate is set to 0.007, and updates the learning rate each epoch by multiplying with learn rate drop factor 0.9.

The test data set signals, also called observation signals Y, have the same initial frequency and chirp rate as training data set and validation data set, but the range of SNR is about from -13dB to -3dB at an interval of 1dB, in total of 11 SNR levels. At each combination of initial frequency and chirp rate, we randomly generate 10 test signals around the same SNR. Test data set size is 3960 signals.

We calculate the SNRs of input Y and DCNN output $\hat{Y}$, the result is illustrated in Fig.3. We can obviously see that after DCNN denoising, the SNRs of $\hat{Y}$ are all increased above 10dB compared to observation Y. Although we train the DCNN at low SNR conditions, which is about from -13dB to -9dB, DCNN also have an ability of filtering at high SNR scenarios. But the variance is deferent between low SNRs and high SNRs. The reason that variance at low SNR levels is relative high is due to the strong noises are randomly distributed, and attenuate the signal structured features that DCNN can extract. DCNN denoising instance is shown in Fig.4 and Fig.5, we can see that DCNN can effectively filter the unstructured noises and output highly structured signal.

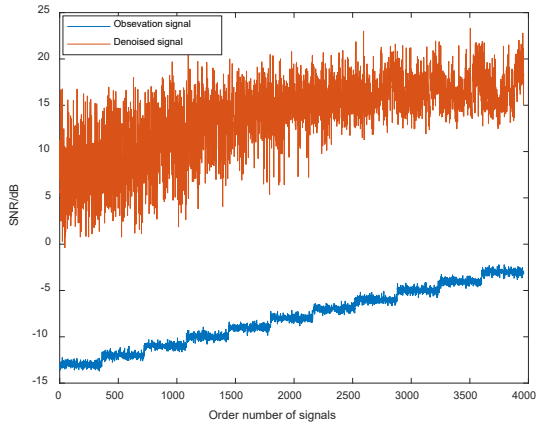

Fig.3. Comparison of SNR between observation signals and denoised signals

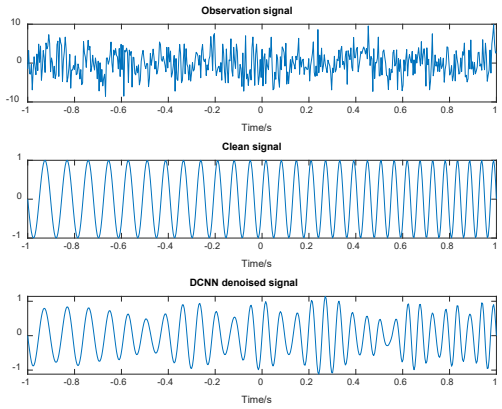

Fig.4. DCNN denoise instance at SNR=-13.3133dB

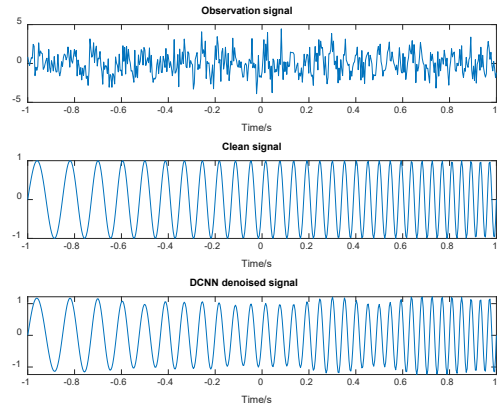

Fig.5. DCNN denoise instance at SNR=-4.8159dB

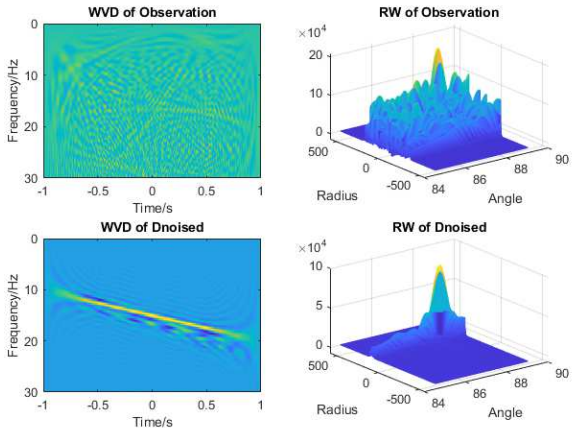

Fig.6. WVD and RW of observation and denoised signal at SNR=-13.3133dB

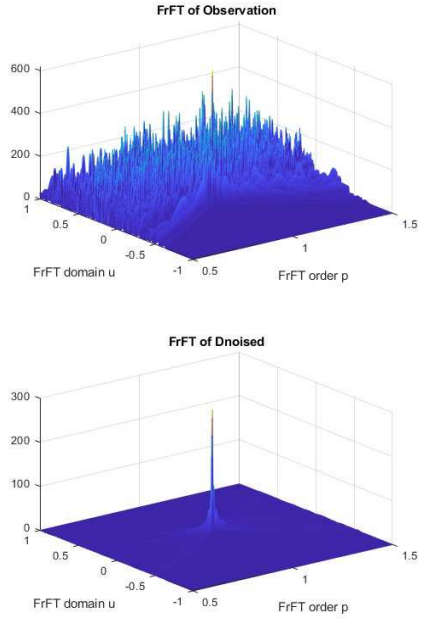

Fig.7. FrFT of observation and denoised signal at SNR=-13.3133dB

The clean chirp signal without noises with initial frequency f_0 and chirp rate k is denoted as Y_c, and parameter estimation result of Y_c is $f_0{}'$ and k', used as truth-value. Parameter estimation result of DCNN output $\hat{Y}$ is $\hat{f}_0$ and $\hat{k}$. Estimation accuracy between Y_c and $\hat{Y}$ is measured by Root Mean Squared Error (RMSE), which is defined as:

$$RMSE_{f_0} = \sqrt{\frac{1}{M}\sum_{i=1}^{M}(f_{0_i}{}' - \hat{f}_{0_i})^2} \quad (17)$$

$$RMSE_k = \sqrt{\frac{1}{M}\sum_{i=1}^{M}(k_i{}' - \hat{k}_i)^2} \quad (18)$$

Where M is the number of test signals.

The RMSE_{f_0} and RMSE_k estimated separately by RW and FrFT are shown in Fig.8 and Fig.9. We can see that with the increase of SNR, the RMSE is descending, and RMSE of $\hat{Y}$ is significantly improved to a great extent compared to observation signals Y. Besides the improvement of filtering performance, from RMSE curve we can also conclude that DCNN trained with low SNR have a good performance in high SNR conditions.

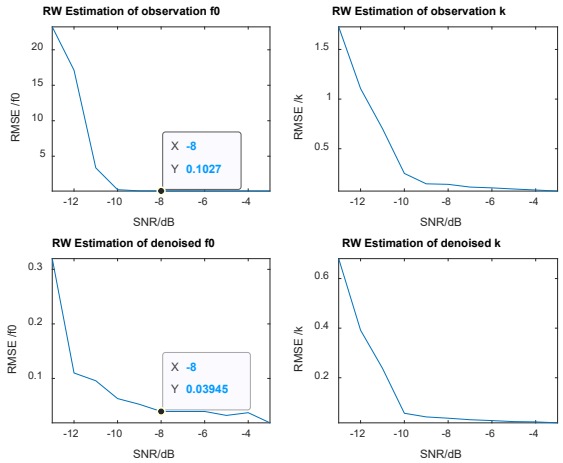

Fig.8. RMSE of f0 and k estimated by RW

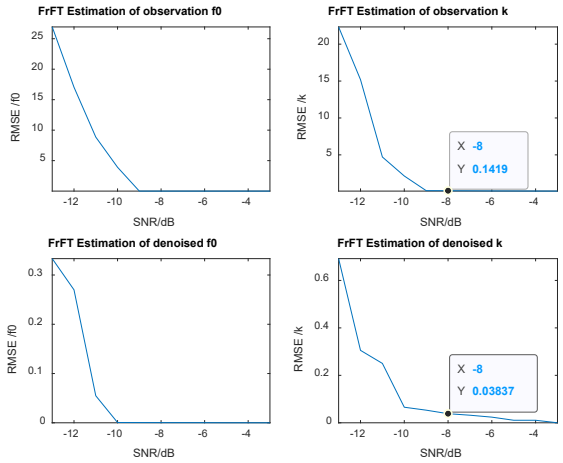

Fig.9. RMSE of f0 and k of by FrFT

Parameter estimation error percentage is defined by following formula:

$$Error\ Quantity\% = \frac{Quantity\ of\ Wrong\ Estimation\ Results}{Quantity\ of\ Total\ Estimation\ Results}\ \% \quad (19)$$

Wrong estimation result is the parameter that the bias is greater than the threshold relative to the parameter of $\mathrm{Y_c}$.

We calculate error percentage at threshold=0.05 and threshold=0.15, the result is shown in Fig.10 and Fig.11. From the curve we can conclude that after DCNN denoising process, parameter estimation accuracy is markedly improved. But at low SNR circumstance, there are also considerable observation signals cannot be processed commendable, the error percentage seems to be acceptable at SNR above -10dB.

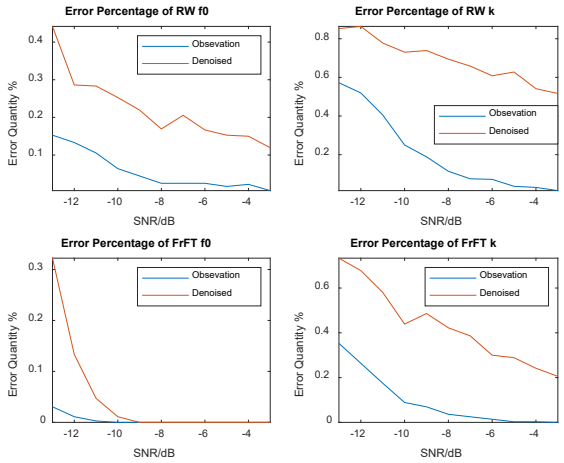

Fig.10. Parameter estimated error percentage at threshold=0.05

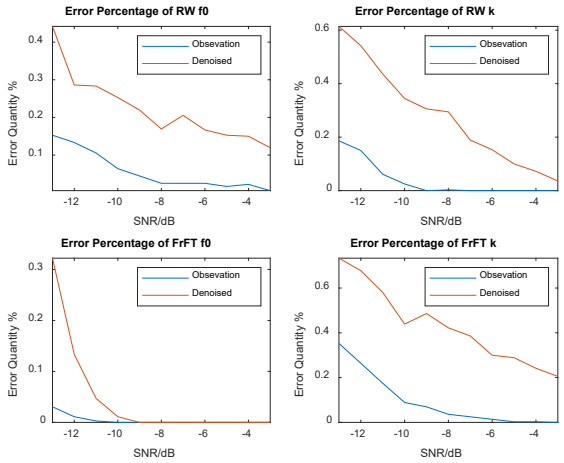

Fig.11. Parameter estimated error percentage at threshold=0.15

4 Conclusions

In this paper, a DCNN based method for filtering chirp signal is proposed. It takes advantage of deep learning feature extraction ability to recover the clean chirp signals as far as possible. Simulation result indicate that DCNN have a good filtering performance at low SNR circumstances, And although DCNN has learned the features of chirp signals at low SNR scenarios, it still work in high SNR conditions. But when the SNR is low enough, DCNN's performance become uncommendable. For future research, we will find solutions to let CNN abstract features in different noise environment and noise types, which will not only be trained in time domain, but also in frequency domain.

Abbreviations

DCNN: Denoising convolutional neural network.
SNR: Signal noise ratio.
CNN: Convolutional neural network.
FrFT: Fractional Fourier transform.
RW: Radon-Wigner Ville transform.

Acknowledgements

The authors would like to thank the anonymous referees for providing valuable suggestions which helped clarify the exposition of the material. Furthermore, the authors would like to thank participants for many fruitful discussions, in particular about the DCNN structure.

Funding

This work was supported by the National Natural Science Foundation of China under Grant 11703027.

Availability of data and materials

Dates used for training/validation/test are generated ourselves. Please contact author for data requests.

Competing interests

The authors declare that they have no competing interests.

Ethics Approval and Consent to Participate

The work described has not been submitted elsewhere for publication, in whole or in part, and all the authors listed have approved the manuscript that is enclosed. I have read and have abided by the statement of ethical standards for manuscripts submitted to EURASIP.

Authors' contributions

GuangliBen developed and implemented the core concepts of the algorithm presented within this manuscript. XifengZheng and YongchengWang provided refinements and performed data acquisition and generation as well as further supplemental programming. XinZhang and NingZhang provided further technical knowledge and support. All authors read and approved the final manuscript.

Authors' information

*** Corresponding author**:Guangli Ben

Guangli Ben received his bachelor's degree in 2013 and master's degree in 2016 from Harbin Engineering University. And he is currently a Ph. D. student and a research assistant at Changchun Institute of Optics, Fine Mechanics and Physics, Chinese Academy of Sciences, Changchun, China. His research interests include digital signal processing, embedded system of space payload. **E-mail addresses:** g2009051126@163.com

Xifeng Zheng received his bachelor's degree in 1991 and Ph. D. degree

from Chinese Academy of Sciences in 2000. He is a researcher of Changchun Institute of Optics, Fine Mechanics and Physics, Chinese Academy of Sciences, Changchun, China. His research interests include image engineering, Liquid crystal and display. **E-mail addresses:** zhengxf@ccxida.com

YONGCHENG WANG received his bachelor's degree from Jilin University in 2003 and Ph. D. degree from Chinese Academy of Sciences in 2010. He is a researcher of Changchun Institute of Optics, Fine Mechanics and Physics, Chinese Academy of Sciences, Changchun, China. His research interests include artificial intelligence, image engineering, and embedded system of space payload. **E-mail addresses:** wyc_dyy@sina.com

XIN ZHANG received her bachelor's degree from Northeastern University, Qinhuangdao, China, in 2016. She is now a Ph. D. candidate at Changchun Institute of Optics, Fine Mechanics and Physics, Chinese Academy of Sciences, Changchun, China. Her research interests cover deep learning and hyperspectral image classification. **E-mail addresses:** zhangxin162@mails.ucas.ac.cn

NING ZHANG received her bachelor's degree from Northeastern University, Qinhuangdao, China, in 2017. She is currently a PhD student at Changchun Institute of Optics, Fine Mechanics and Physics, Chinese Academy of Sciences, Changchun, China. Her research interests cover image processing, deep learning and remote sensing image super-resolution. **E-mail addresses:** zhangning171@mails.ucas.ac.cn

References

[1]. L. A. A. Irkhis and A. K. Shaw, "Compressive Chirp Transform for Estimation of Chirp Parameters," *2019 27th European Signal Processing Conference (EUSIPCO)*, A Coruna, Spain, 2019, pp. 1-5, DOI:10.23919/EUSIPCO.2019.8903119

[2]. K. Czarnecki and M. Moszyński, "A novel method of local chirp-rate estimation of LFM chirp signals in the time-frequency domain," *2013 36th International Conference on Telecommunications and Signal Processing (TSP)*, Rome, 2013, pp. 704-708, DOI:10.1109/TSP.2013.6614028

[3]. Y. Jiang, H. Li and M. Rangaswamy, "Deep Learning Denoising Based Line Spectral Estimation," in *IEEE Signal Processing Letters*, vol. 26, no. 11, pp. 1573-1577, Nov. 2019, DOI**:**10.1109/LSP.2019.2939049

[4]. Liu Ding. Smaragdis Paris. Kim Minje. "Experiments on deep learning for speech denoising". In INTERSPEECH-2014, 2685-2689.

[5]. X. Chen, Q. Jiang, N. Su, B. Chen and J. Guan, "LFM Signal Detection and Estimation Based on Deep Convolutional Neural Network," *2019 Asia-Pacific Signal and Information Processing Association Annual Summit and Conference (APSIPA ASC)*, Lanzhou, China, 2019, pp. 753-758. DOI:10.1109/APSIPAASC47483.2019.9023016.

[6]. H. Jin, W. Li, X. Wang, Y. Zhang, S. Yu and Q. Shi, "Preamble Detection for Underwater Acoustic Communications Based on Convolutional Neural Networks," *2018 OCEANS - MTS/IEEE Kobe Techno-Oceans (OTO)*, Kobe, 2018, pp. 1-6. DOI:10.1109/OCEANSKOBE.2018.8559089.

[7]. J. Brynolfsson and M. Sandsten, "Classification of one-dimensional non-stationary signals using the Wigner-Ville distribution in convolutional neural networks," *2017 25th European Signal Processing Conference (EUSIPCO)*, Kos, 2017, pp. 326-330. DOI:10.23919/EUSIPCO.2017.8081222.

[8]. Ioffe, Sergey, and Christian Szegedy. "Batch normalization: Accelerating deep network training by reducing internal covariate shift."*preprint, arXiv:1502.03167*(2015).

[9]. Kingma, Diederik, and Jimmy Ba. "Adam: A method for stochastic optimization."*arXiv preprint arXiv:1412.6980*(2014).

[10]. S. Saha and S. Kay, "A noniterative maximum likelihood parameter estimator of superimposed chirp signals," *2001 IEEE International Conference on Acoustics, Speech, and Signal Processing. Proceedings (Cat. No.01CH37221)*, Salt Lake City, UT, USA, 2001, pp. 3109-3112 vol.5.. DOI:10.1109/ICASSP.2001.940316.

[11]. Y. Lin, Y. Peng and X. Wang, "Maximum likelihood parameter estimation of multiple chirp signals by a new Markov chain Monte Carlo approach," *Proceedings of the 2004 IEEE Radar Conference (IEEE Cat. No.04CH37509)*, Philadelphia, PA, USA, 2004, pp. 559-562. DOI:10.1109/NRC.2004.1316487.

[12]. S. Saha and S. M. Kay, "Maximum likelihood parameter estimation of superimposed chirps using Monte Carlo importance sampling," in *IEEE Transactions on Signal Processing*, vol. 50, no. 2, pp. 224-230, Feb. 2002. DOI:10.1109/78.978378.

[13]. K. Czarnecki and M. Moszyński, "A novel method of local chirp-rate estimation of LFM chirp signals in the time-frequency domain," *2013 36th International Conference on Telecommunications and Signal Processing (TSP)*, Rome, 2013, pp. 704-708. DOI:10.1109/TSP.2013.6614028.

[14]. K. Ding, Q. Ding and R. Z. Lan, "Parameters estimation of LFM signal based on fractional order cross spectrum," *Proceedings of 2011 International Conference on Electronic & Mechanical Engineering and Information Technology*, Harbin, 2011, pp. 654-656. DOI:10.1109/EMEIT.2011.6022981.

[15]. H. Hang, "Time-Frequency DOA Estimation Based on Radon-Wigner Transform," *2006 8th international Conference on Signal Processing*, Beijing, 2006, pp. DOI:10.1109/ICOSP.2006.344553.

[16]. J. C. Wood and D. T. Barry, "Radon transformation of time-frequency distributions for analysis of multicomponent signals," in *IEEE Transactions on Signal Processing*, vol. 42, no. 11, pp. 3166-3177, Nov. 1994.. DOI: 10.1109/78.330375

[17]. Narayanan, V. & Prabhu, K.M.M.. (2003). "The fractional Fourier transform: Theory, implementation and error analysis. " *Microprocessors and Microsystems.* 27. 511-521. DOI:10.1016/S0141-9331(03)00113-3.

[18]. Y. Ding, L. Sun, H. Zhang and B. Zheng, "A multi-component LFM signal parameters estimation method using STFT and Zoom-FRFT," *2016 8th IEEE International Conference on Communication Software and Networks (ICCSN)*, Beijing, 2016, pp. 112-117. DOI: 10.1109/ICCSN.2016.7586630

Figures

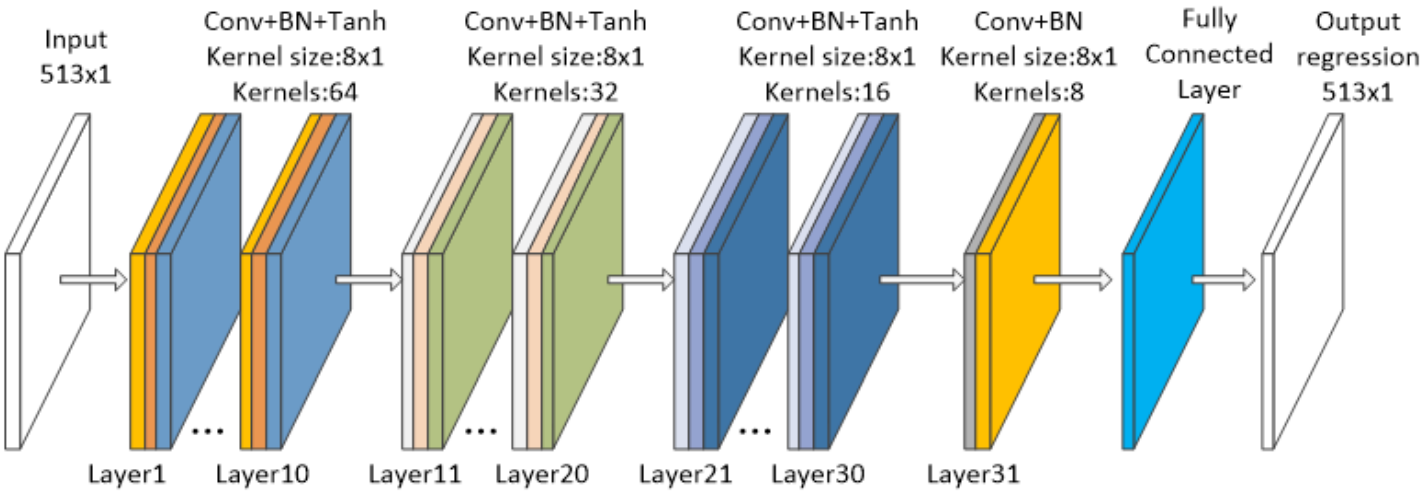

Figure 1

Structure of DCNN

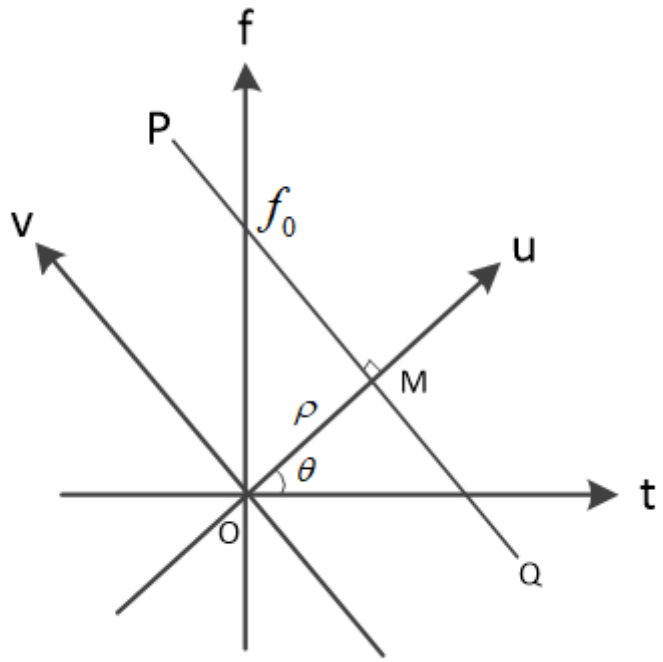

Figure 2

The diagram of Radon transform

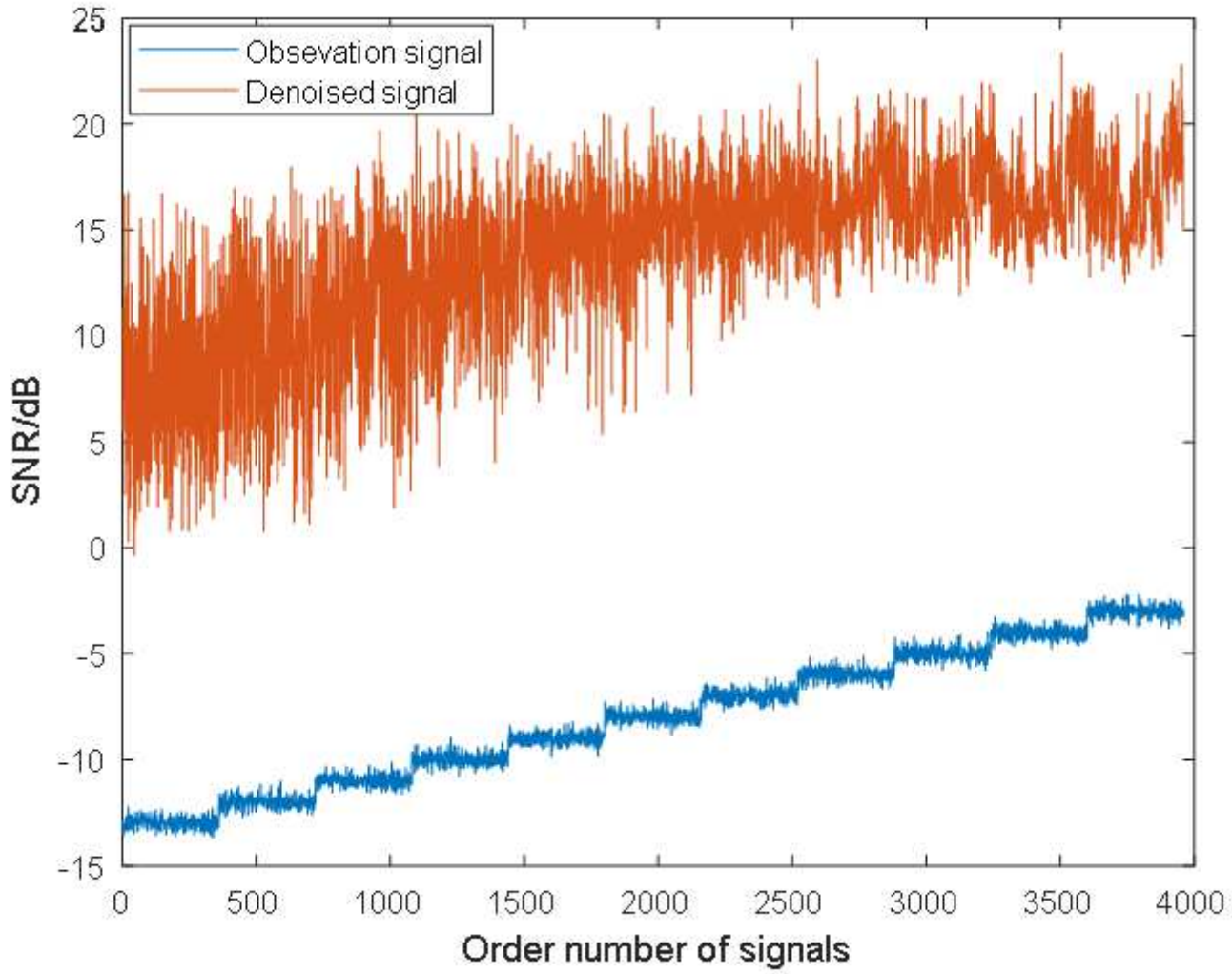

Figure 3

Comparison of SNR between observation signals and denoised signals

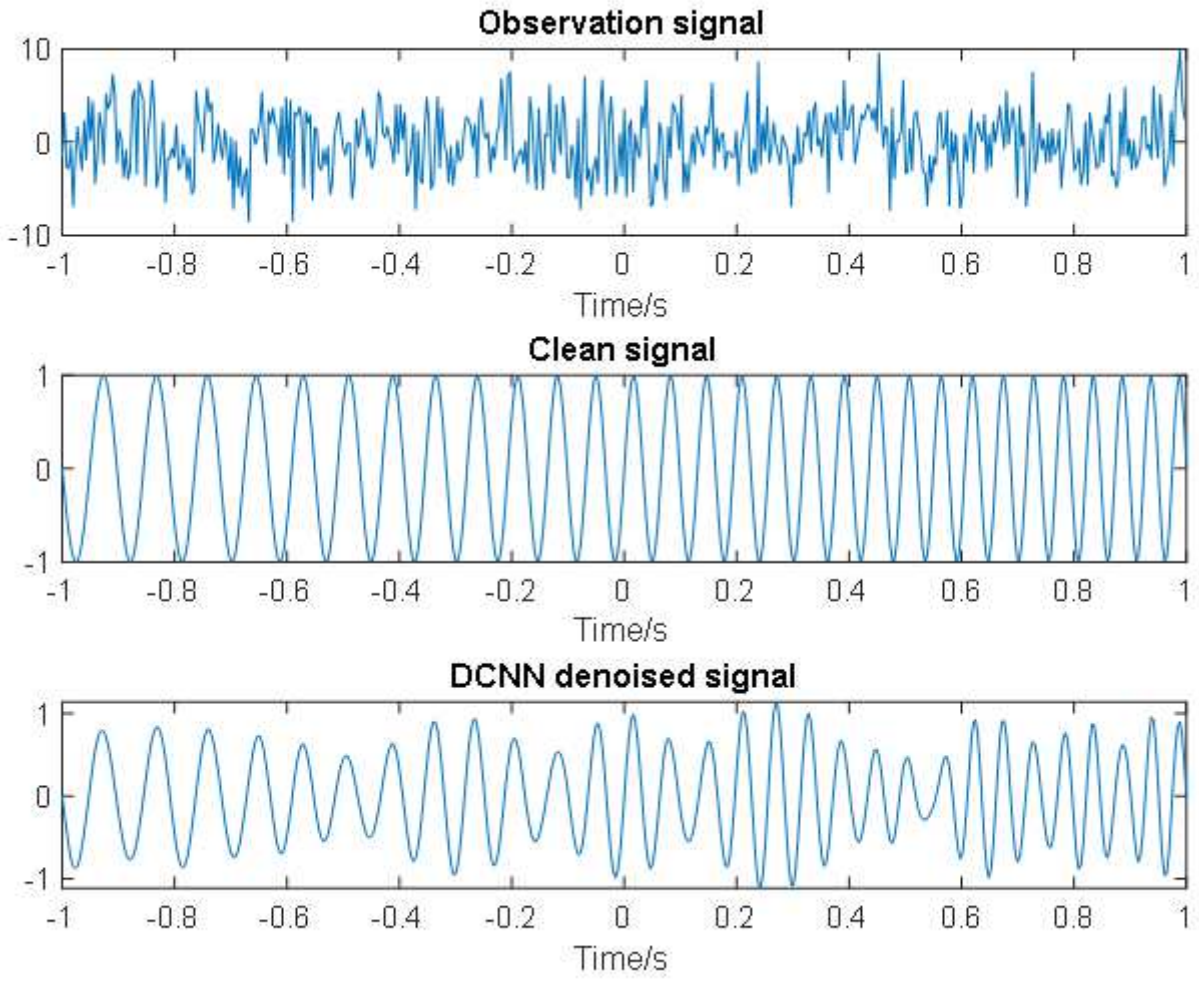

Figure 4

DCNN denoise instance at SNR=-13.3133dB

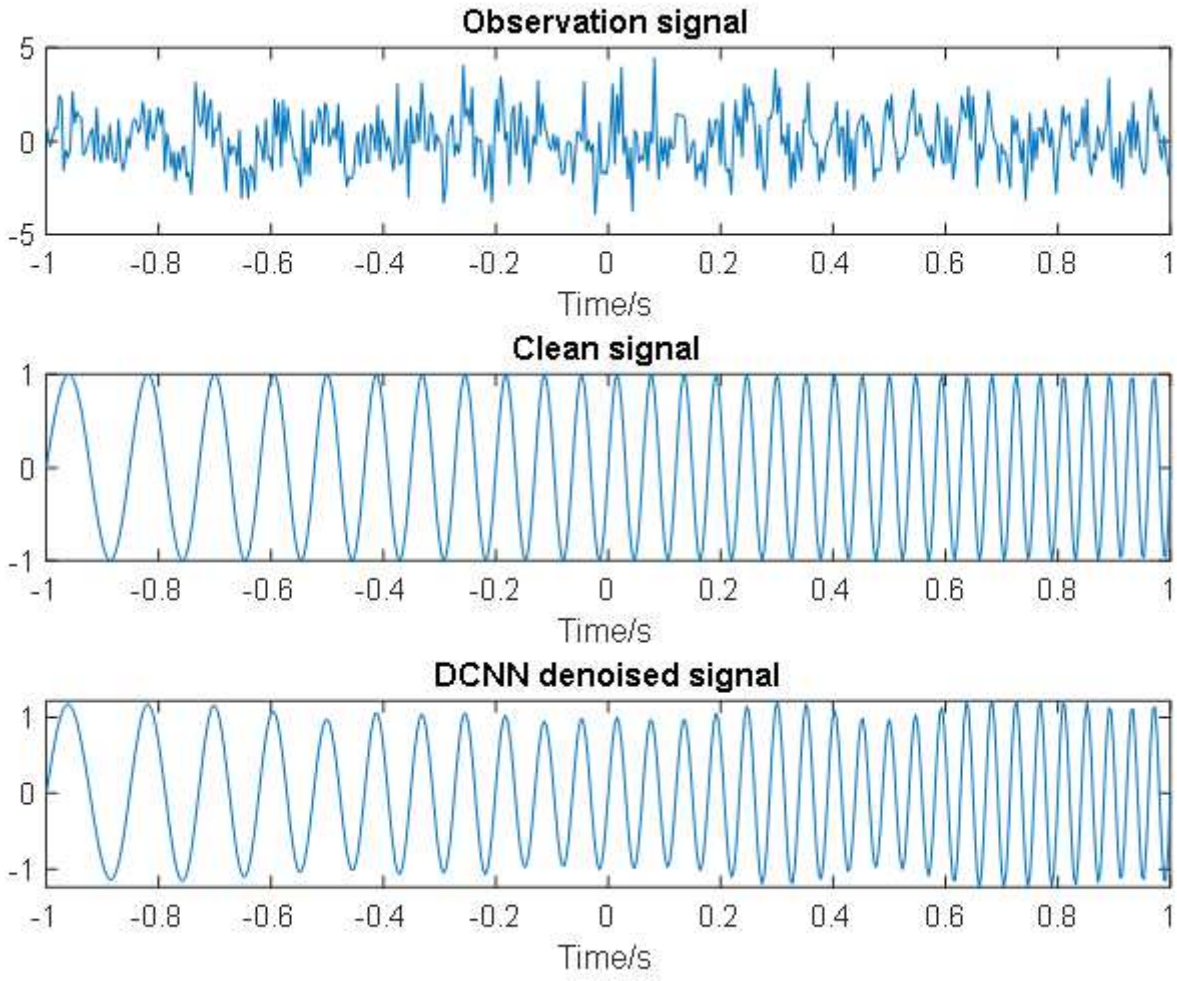

Figure 5

DCNN denoise instance at SNR=-4.8159dB

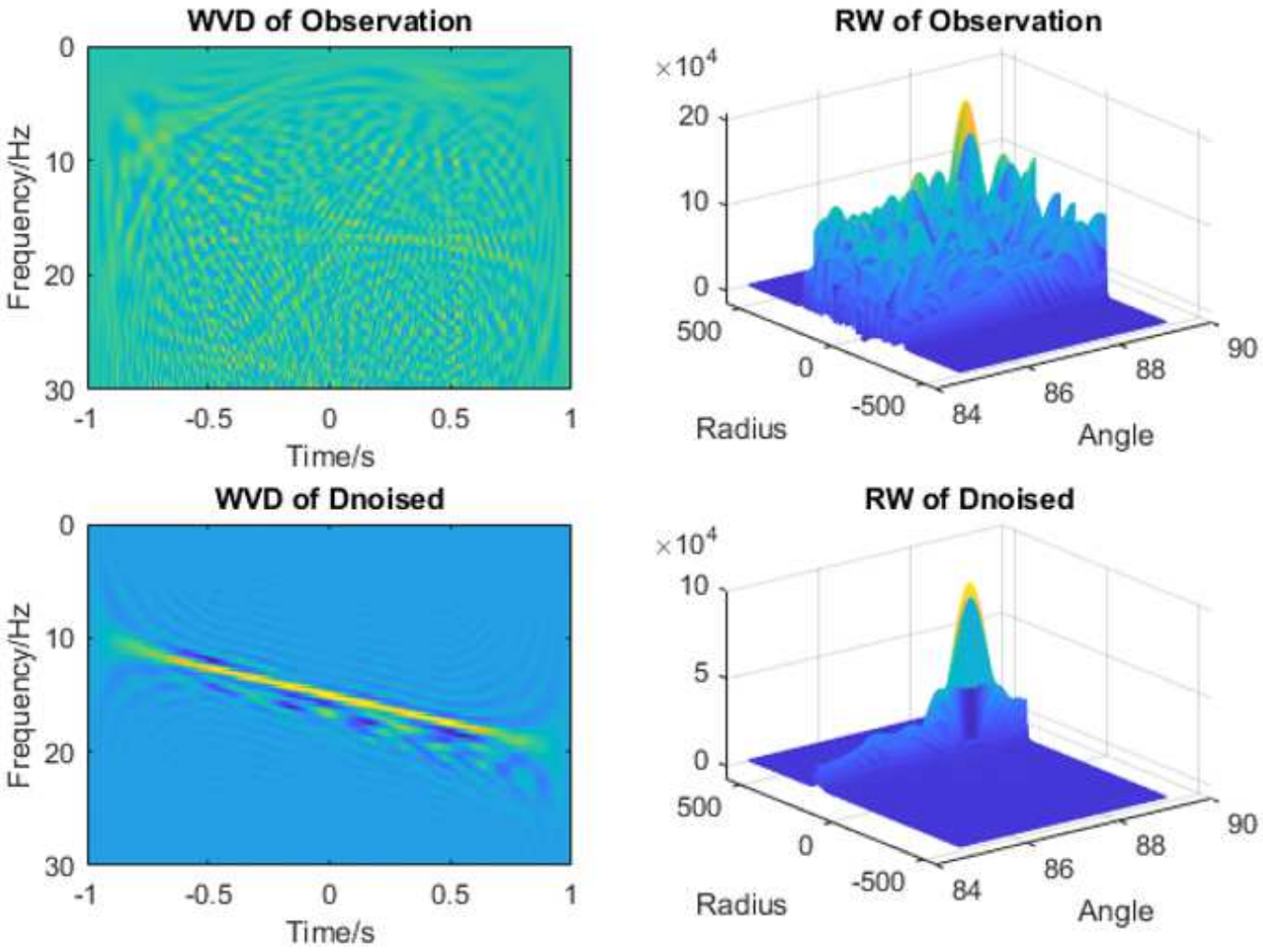

Figure 6

WVD and RW of observation and denoised signal at SNR=-13.3133dB

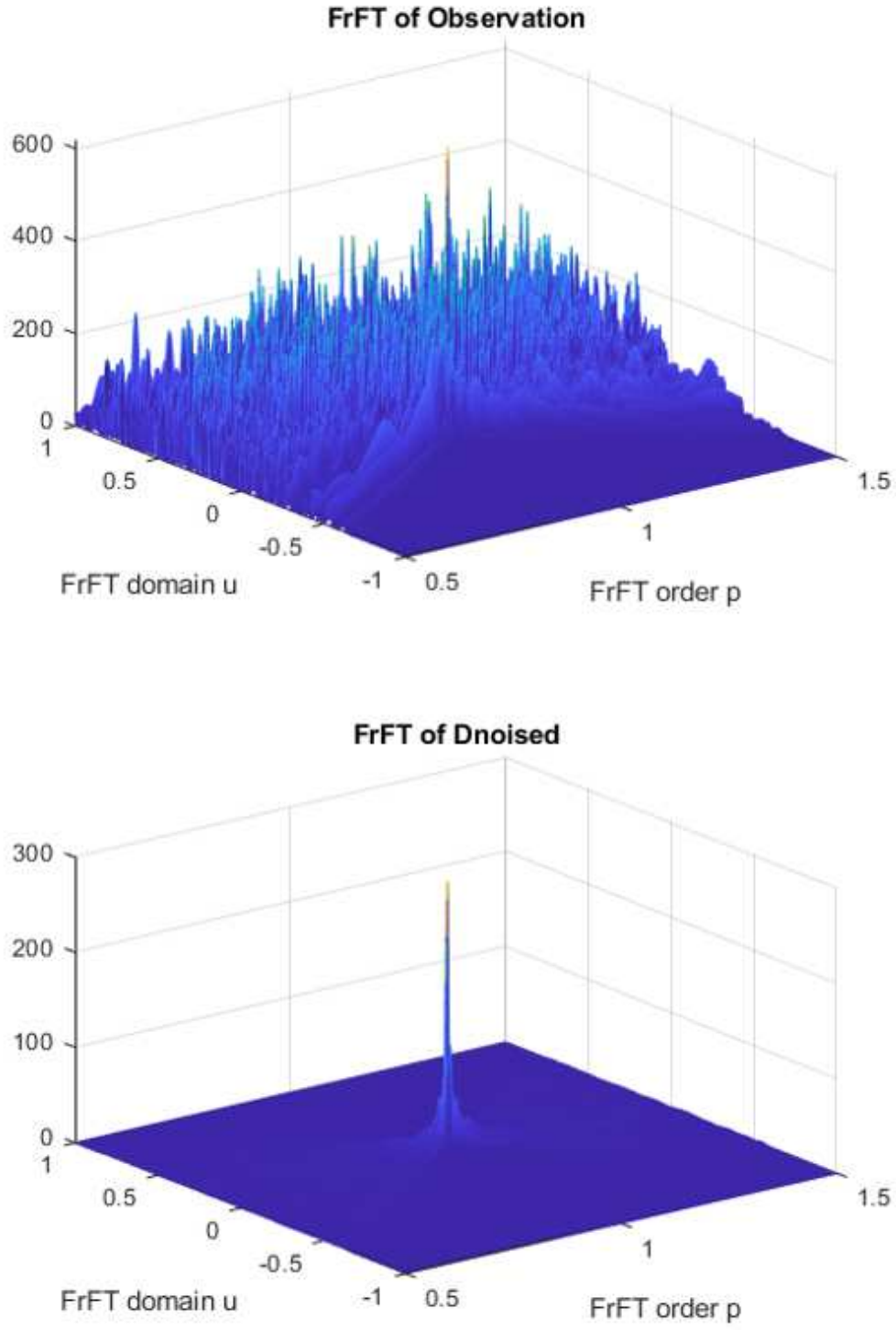

Figure 7

FrFT of observation and denoised signal at SNR=-13.3133dB

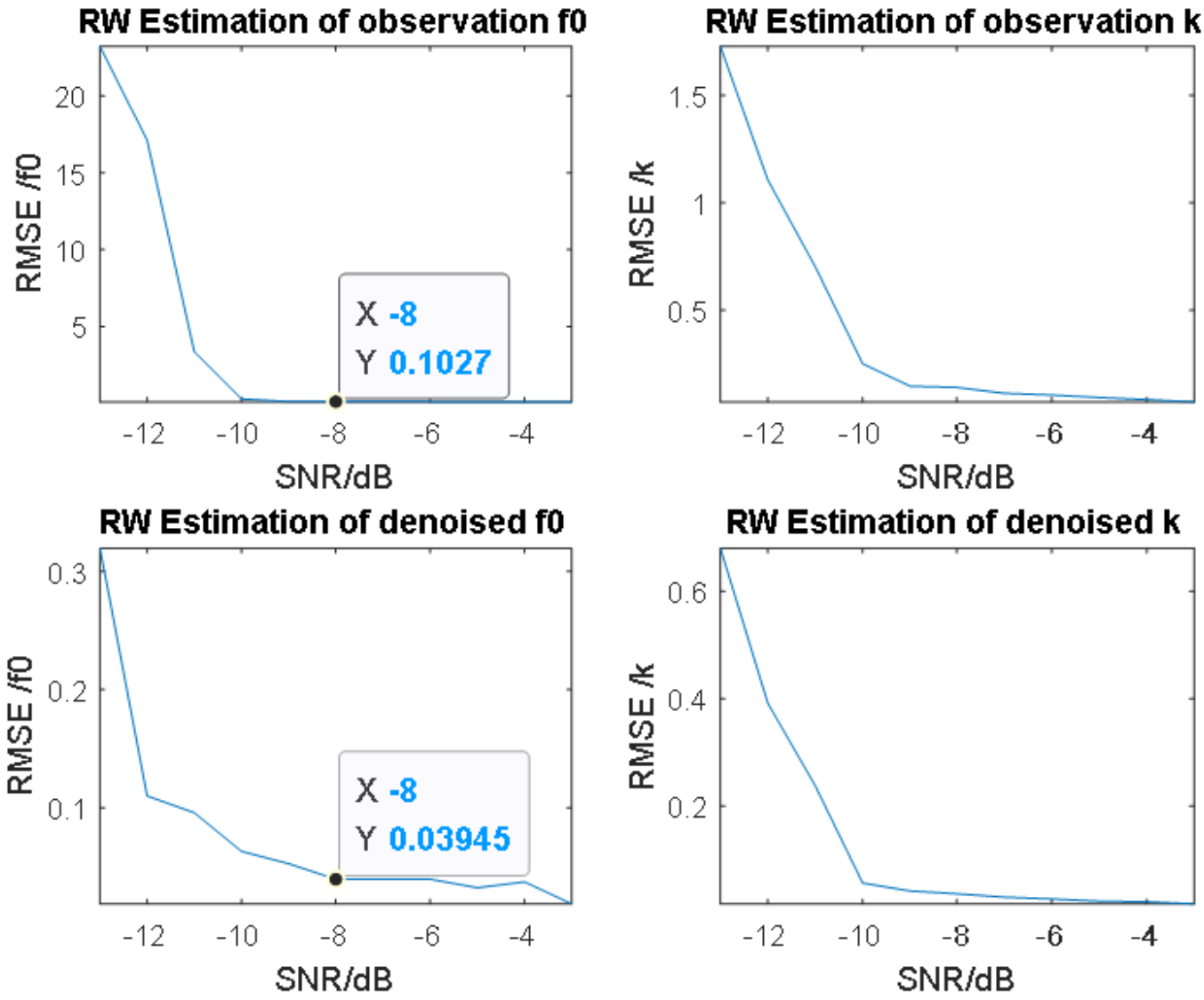

Figure 8

RMSE of f0 and k estimated by RW

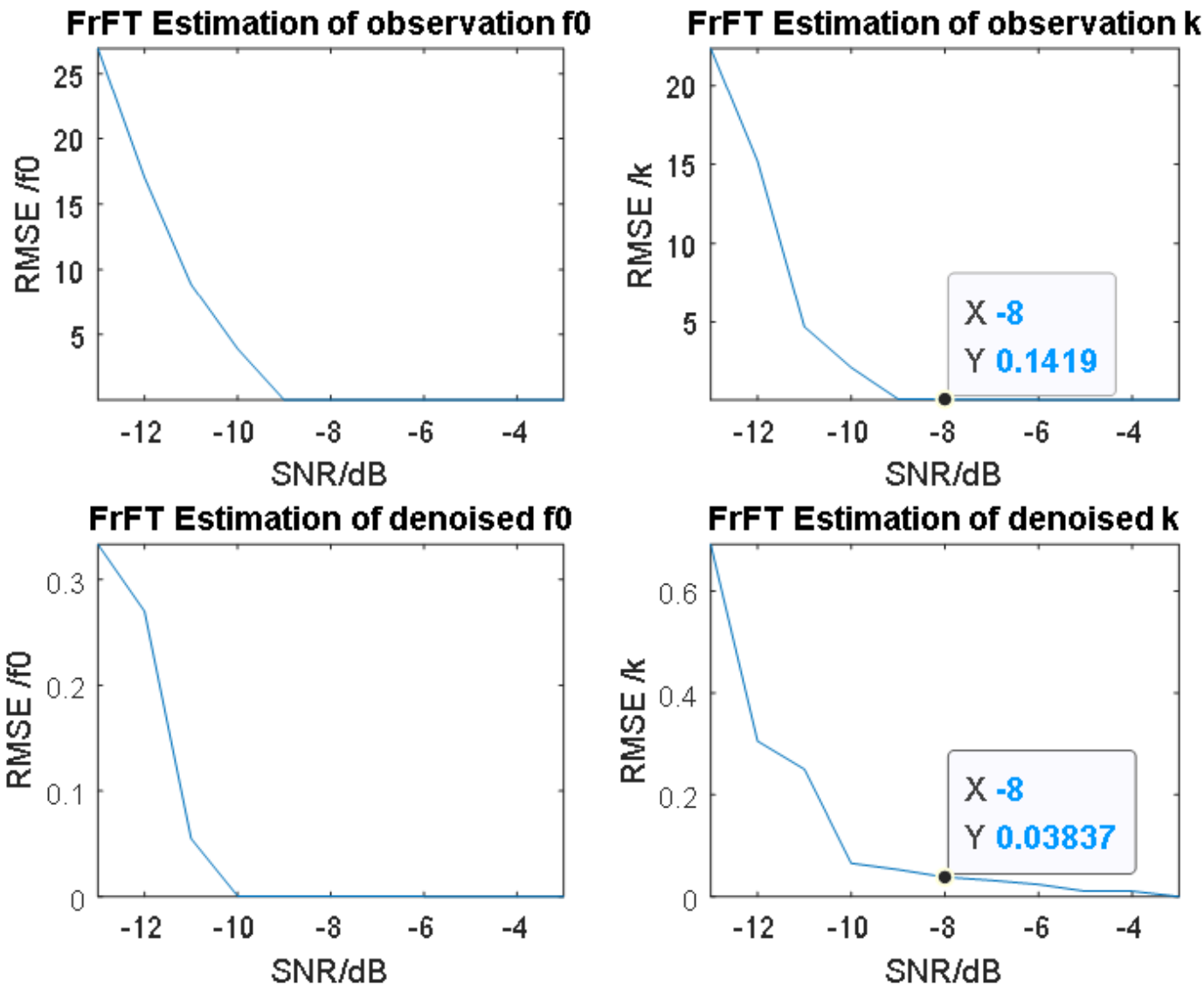

Figure 9

RMSE of f0 and k of by FrFT

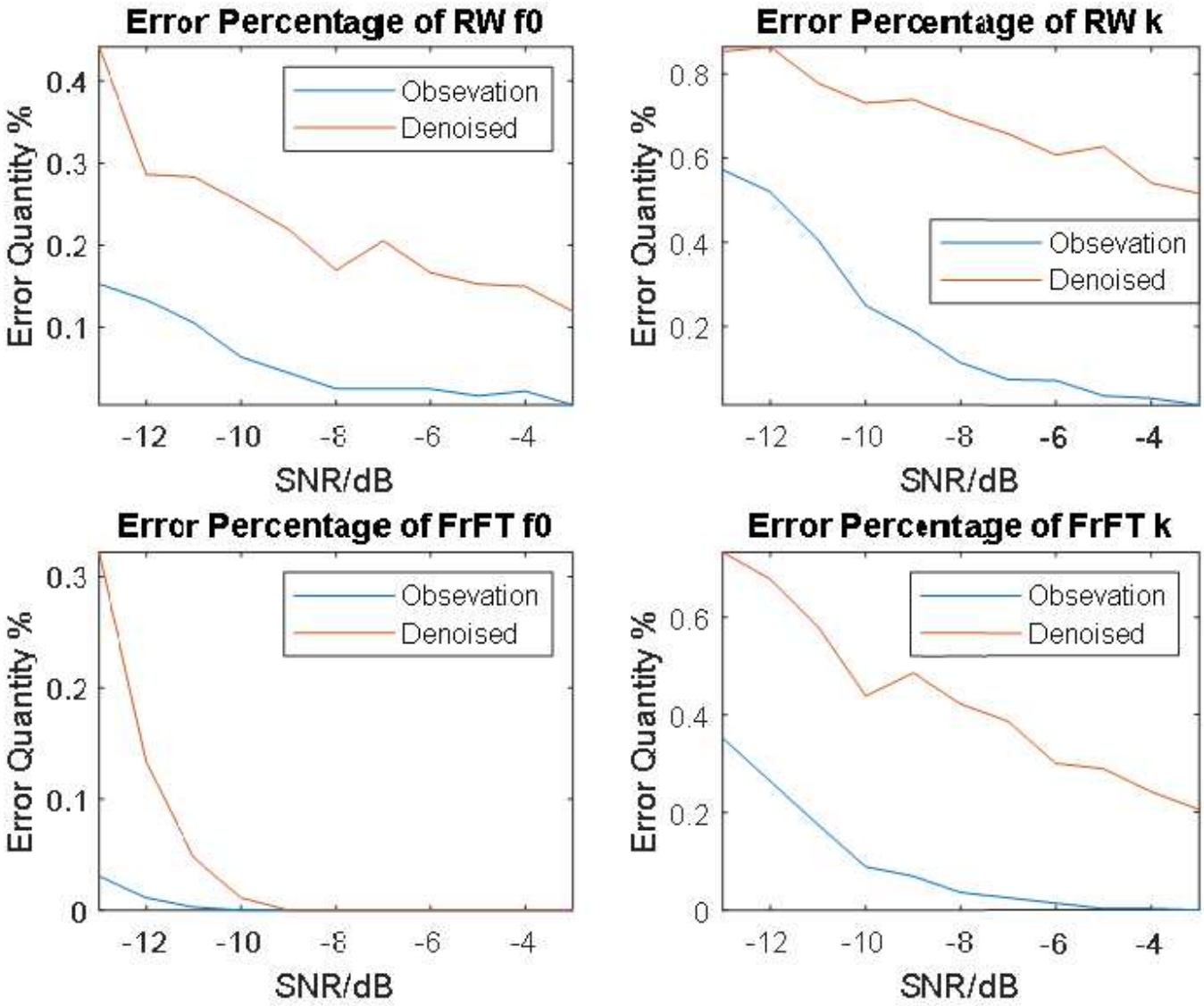

Figure 10

Parameter estimated error percentage at threshold=0.05

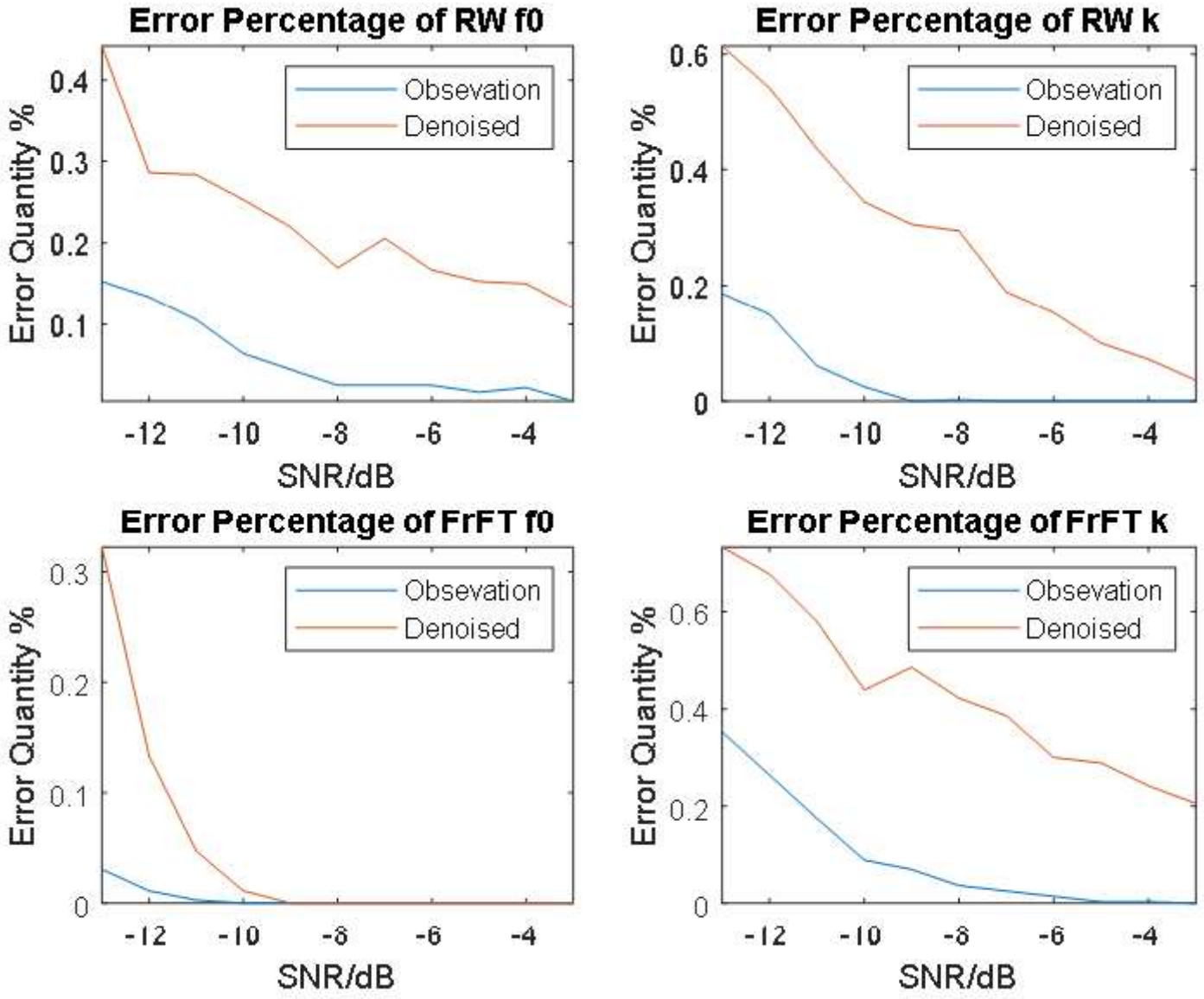

Figure 11

Parameter estimated error percentage at threshold=0.15